Oncogene (2003) 22, 1978–1987

www.nature.com/onc

Evidence of multifocality of telomere erosion in high-grade prostatic intraepithelial neoplasia (HPIN) and concurrent carcinoma

Bisera Vukovic[1,2], Paul C Park[1], Jaudah Al-Maghrabi[1,2], Ben Beheshti[1,3], Joan Sweet[3,4], Andy Evans[3,4], John Trachtenberg[5] and Jeremy Squire[1,2,3]

[1]*Ontario Cancer Institute/Princess Margaret Hospital, The University Health Network, Toronto, Ontario, Canada M5G 2M9;* [2]*Department of Medical Biophysics, Faculty of Medicine, University of Toronto, The University Health Network, Toronto, Ontario, Canada M5G 2M9;* [3]*Laboratory Medicine and Pathobiology, Faculty of Medicine, University of Toronto, The University Health Network, Toronto, Ontario, Canada M5G 2M9;* [4]*Division of Pathology, Faculty of Medicine, University of Toronto, The University Health Network, Toronto, Ontario, Canada M5G 2M9;* [5]*Divison of Urology, Faculty of Medicine, University of Toronto, The University Health Network, Toronto, Ontario, Canada M5G 2M9*

Mechanisms underlying prostate cancer (CaP) initiation and progression are poorly understood. A chromosomal instability mechanism leading to the generation of numerical and structural chromosomal changes has been implicated in the preneoplastic and neoplastic stages of CaP. Telomere dysfunction is one potential mechanism associated with the onset of such instability. To determine whether there was alteration in telomere length and chromosome number, 15 paraffin-embedded prostatectomy specimens were investigated using quantitative peptide nucleic acid (PNA) FISH analysis of representative foci of carcinoma, putative precancerous lesions (high-grade prostatic intraepithelial neoplasia, HPIN) and nondysplastic prostate epithelium. A significant decrease in telomere length was shown in both HPIN and CaP in comparison with normal epithelium. In addition, elevated rates of aneusomy suggested that increased levels of chromosomal aberrations were associated with decreased telomere length. Moreover, multiple foci of HPIN were shown to have a heterogeneous overall reduction of telomere length. This reduction was more evident in the histologic regions of the prostate containing CaP. Such observations lend support to the hypothesis that telomere erosion may be a consistent feature of CaP oncogenesis and may also be associated with the generation of chromosomal instability that characterizes this malignancy.
Oncogene (2003) **22,** 1978–1987. doi:10.1038/sj.onc.1206227

Keywords: prostate; telomere; heterogeneity

Introduction

Prostate cancer (CaP) is the most frequently diagnosed form of cancer in men in North America although the etiology of CaP remains largely unknown (Haas and Sakr, 1997). Multistep accumulation of genetic aberrations ultimately leading to a malignant phenotype is thought to underlie disease progression (Isaacs *et al*., 1994; Dong *et al*., 1997). High-grade prostatic intraepithelial neoplasia (PIN) (HPIN) has been extensively studied and is currently considered the most likely precursor to invasive prostatic adenocarcinoma (McNeal and Bostwick, 1986; Graham *et al*., 1992; van der Kwast *et al*., 1999). It is characterized by a proliferation of secretory prostatic epithelial cells that have malignant morphology, with a discontinuous basal cell layer and absence of demonstrable invasion. HPIN and CaP frequently coexist and tend to be multifocal (Sakr *et al*., 1993, 1996; Bastacky *et al*., 1995; Emmert-Buck *et al*., 1995; Bostwick *et al*., 1998; Sakr and Grignon, 1998). The incidence of HPIN increases with age and is more frequently observed in men at higher risk for developing CaP such as African-Americans (Muir *et al*., 1991; Sakr *et al*., 1995, 1996).

In support of the idea that the HPIN is a precursor lesion to CaP, both the chromosomal and genetic changes observed in HPIN are similar to those seen in primary and metastatic CaP (Qian *et al*., 1999). Fluorescence *in situ* hybridization (FISH) and comparative genomic hybridization (CGH) studies have shown increase in DNA ploidy in HPIN and prostate cancer. Loss of 8p and gain of 8q were the most frequent changes followed by gain of chromosomes 7, 10q, 16q and 18q (Macoska *et al*., 1994; Qian *et al*., 1995; Erbersdobler *et al*., 1996; Takahashi *et al*., 1996; Sakr and Partin, 2001). There is increasing evidence that acquisition of numerical and structural chromosomal alterations observed in CaP and HPIN could be a consequence of an underlying process of chromosomal segregation errors, and a more general underlying process of genomic instability (Al-Maghrabi *et al*., 2001; Beheshti *et al*., 2001).

Telomeres are specialized structures that cap the ends of linear chromosomes and are essential for maintaining chromosomal stability. Natural shortening of telomeres with each cell division has been postulated to serve as a mitotic clock (Olovnikov, 1973; Harley, 1991; Counter, 1996), limiting the replicative potential of the cell. This

*Correspondence: Jeremy Squire, Ontario Cancer Institute, The University Health Network, 610 University Avenue, Toronto, Ontario, Canada M5G 2M9; E-mail: jeremy.squire@utoronto.ca
Received 29 August 2002; revised 8 November 2002; accepted 0 November 2002

shortening has been hypothesized as a protective mechanism against indefinite proliferation of preneoplastic cells (Counter, 1996; Goyns and Lavery, 2000).

Excessive telomere shortening leads to telomere dysfunction, end-to-end chromosome fusion, rearrangements and ultimately cell death (Muller, 1938; McClintock, 1941; Ducray *et al*., 1999; Hande *et al*., 1999; Artandi and DePinho, 2000). For continuing proliferation, the cell must reactivate telomerase or stabilize telomeres by some alternative pathway (Wen *et al*., 1998; Grobelny *et al*., 2001). High levels of telomerase activity (80–90%) were reported in CaP and were found to vary in HPIN (15–85%) (Kallakury *et al*., 1997; Lin *et al*., 1997; Scates *et al*., 1997; Takahashi *et al*., 1997; Koeneman *et al*., 1998; Zhang *et al*., 1998; Wullich *et al*., 1999). Although stabilization of telomeres may prevent further chromosomal fusions, the telomeres remain short in majority of cancers including CaP.

In this study, an established quantitative fluorescence *in situ* hybridization (Q-FISH) method (Poon *et al*., 1999), previously applied using formalin-fixed paraffin-embedded histologic sections (Meeker *et al*., 2002), was employed to assess changes in telomere length, chromosomal aneusomy and proliferative activity in HPIN and CaP in comparison with nondysplastic prostatic epithelium. In addition, aneusomy levels and p53 status were correlated in a subset of samples to determine whether there was concordance between parameters of genomic instability and telomere erosion.

Results

Analysis of telomere length

To measure the relative changes in telomere length in prostate epithelium, the established technique of Q-FISH with telomere-specific PNA probes was utilized (Poon *et al*., 1999). The relative amount of PNA probe hybridizing to the telomeric end has been shown to be directly proportional to the length of the telomeric DNA tract. The brightest signals were visualized, while smaller telomeric signals fell below background levels of fluorescence, thus limiting the analysis to comparison of relative changes in telomere fluorescence between areas of interest rather than absolute length measurements. Using this approach, cell-to-cell topographical variation of telomere and centromere signal intensities in distinct epithelial histologies of the diseased tissue was analysed free of undesirable contaminants from surrounding stroma or basal epithelial cell layer.

The characteristics of the study group are listed in Table 1. For each patient, representative areas of carcinoma, HPIN and benign tissue were analysed. The analysis focused on the secretory epithelial layer (Figure 1a,b), since this layer is thought to give rise to majority of prostate adenocarcinomas. A marked reduction in telomeric signal number and intensity in HPIN and CaP cells compared to benign epithelium was observed (Figure 1c,d). Quantitative analysis of averaged telomere fluorescence intensities from 15 specimens resulted in the intensity profiles in Figure 2a. On average, an 85% reduction in total signal intensity was observed in CaP relative to the nondysplastic prostate epithelium. Telomere signals in HPIN were found to vary considerably in individual foci, and to differ with respect to their proximity to carcinoma. HPIN lesions that were situated immediately adjacent to CaP (less than 2 mm distance) or intermingled with CaP (Figure 3), on average, displayed a mean reduction in total telomere signal intensity of 68% in comparison with normal epithelium. In contrast, HPIN foci situated away from CaP exhibited a more closely matched telomere signal intensity to benign epithelium, with a mean of 32% reduction in total signal intensity (Table 1).

Table 1 Clinical data with the corresponding interphase FISH analysis of patient material ($n=15$)[a]

Case	*Age*	*Numerical abnormalities* (chromosomes 7,8 and Y)	*Gleason Score*	*Telomere intensity*				*Centromere intensity*			
				CaP	*HPIN near CaP*	*HPIN away from CaP*	*Normal epithelium*	*CaP*	*HPIN near CaP*	*HPIN away from CaP*	*Normal epithelium*
1	57	8+	6	0.622	1.137	3.343	5.191	116843.6	99832.0	81347.0	72349.1
2	70	8+	6	1.312	2.034	3.427	4.451	110942.8	94556.8	100574.9	82497.5
3	51	7+,8+	10	0.352	1.293	3.587	3.628	93781.3	98956.6	95761.4	39265.3
4	61	N[b]	6	0.527	0.682	2.531	4.725	94437.1	129343.4	134190.1	50679.6
5	66	N	6	0.787	1.235	2.462	4.529	112279.9	67841.2	79938.1	34467.1
6	56	N	6	0.986	0.871	2.552	4.946	103481.0	71843.5	127184.5	67191.2
7	67	ND[c]	7	0.827	1.344	4.136	3.958	93714.2	72459.6	85063.1	57184.0
8	71	ND	6	0.378	0.763	1.807	4.568	96345.5	91348.5	48273.5	38997.1
9	70	ND	6	0.629	0.642	1.707	5.244	37581.4	84964.9	76770.5	20250.8
10	69	ND	7	0.569	1.295	4.649	3.924	103616.2	81467.9	97143.1	64784.1
11	61	N	7	0.814	2.841	3.126	4.385	97204.4	67983.6	51374.1	43671.4
12	63	N	7	0.465	2.903	3.384	5.063	136290.6	106302.1	76877.9	64398.0
13	63	ND	6	0.519	2.316	4.103	3.132	82232.5	80994.9	94315.7	50488.2
14	55	ND	7	0.42	0.897	1.885	3.384	128441.2	105848.9	116942.3	109633.2
15	53	ND	6	0.939	0.825	2.452	5.536	71164.0	109842.5	119346.8	48341.5

[a]Supplementary data including s.d., number of cells counted for each region and additional sample information are available at www.utoronto.ca/cancyto/supplement. [b]Normal (diploid). [c]Not determined

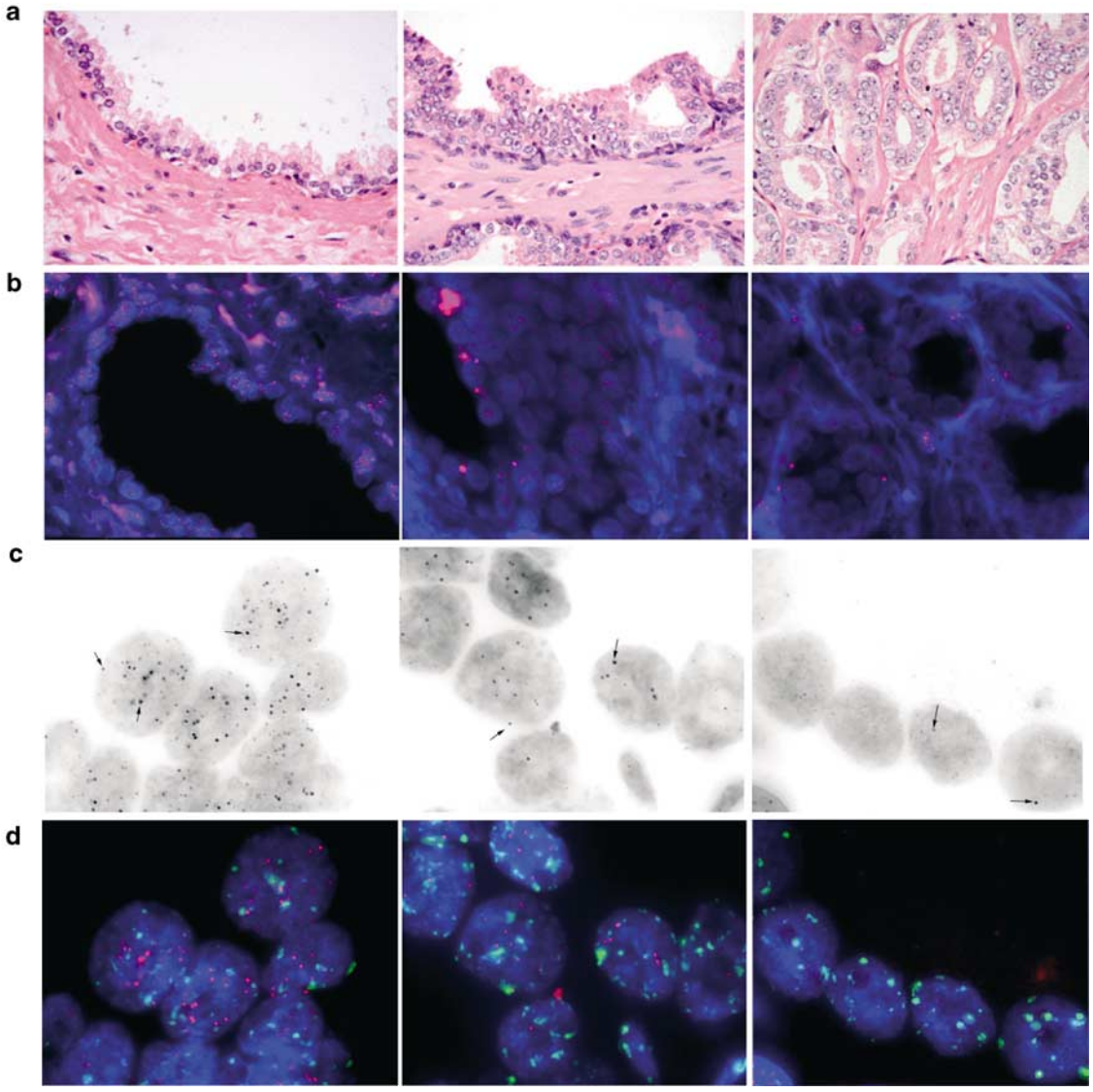

Figure 1 Parallel H&E sections shown in (**a**) were used to determine regions of interest. (**b**–**d**): FISH with centromeric (FITC-green) and telomeric (Cy3-red) PNA probes on paraffin-embedded tissue sections with X40 (**b**) and $\times 100$ (**c**–**d**) objective. Representative images of benign tissue, HPIN and CaP are shown in each row (left to right, respectively). DAPI was used as a counterstain. Identical images in B&W are shown in (**c**) with nuclei outlined in gray and telomere signals represented by the dark spots (indicated by arrows). Note reduction in telomere signal intensity and size in HPIN and CaP in comparison with benign tissue

Statistical analysis of telomere length

Analysis of variance (ANOVA) was performed followed by a Student–Newman–Keuls (SNK) test to ascertain whether the reduction in telomeric signals was statistically significant. The reduction of telomere signal in CaP foci compared to normal epithelium was found to be significant in all the 15 patients ($P<0.05$). Variance in telomere intensities was found to be higher on an intrapatient than interpatient basis. Consequently, ANOVA analysis was also performed on a per patient basis to confirm that differences in averaged intensities were significant on a single patient level. In 12 out of 15 patients, HPIN situated near CaP demonstrated significant signal reduction ($P<0.05$). This trend was less apparent in HPIN situated away from CaP with only seven out of 15 patient samples exhibiting significant signal reduction relative to benign epithelium.

Analysis of aneusomy, p53 levels and Ki-67

In parallel, total centromere intensities were analysed on a per cell basis resulting in the profile shown in Figure 2b. Centromere intensities averaged over 15 specimens demonstrated a 75% increase in total centromere intensity in both CaP and HPIN compared to benign tissue. No significant change in centromere intensities was found between carcinoma and different HPIN foci. As described above, ANOVA and an SNK test were used to confirm this trend in all tissue samples in the study group. Eight out of 15 samples analysed showed significantly different ploidy changes from

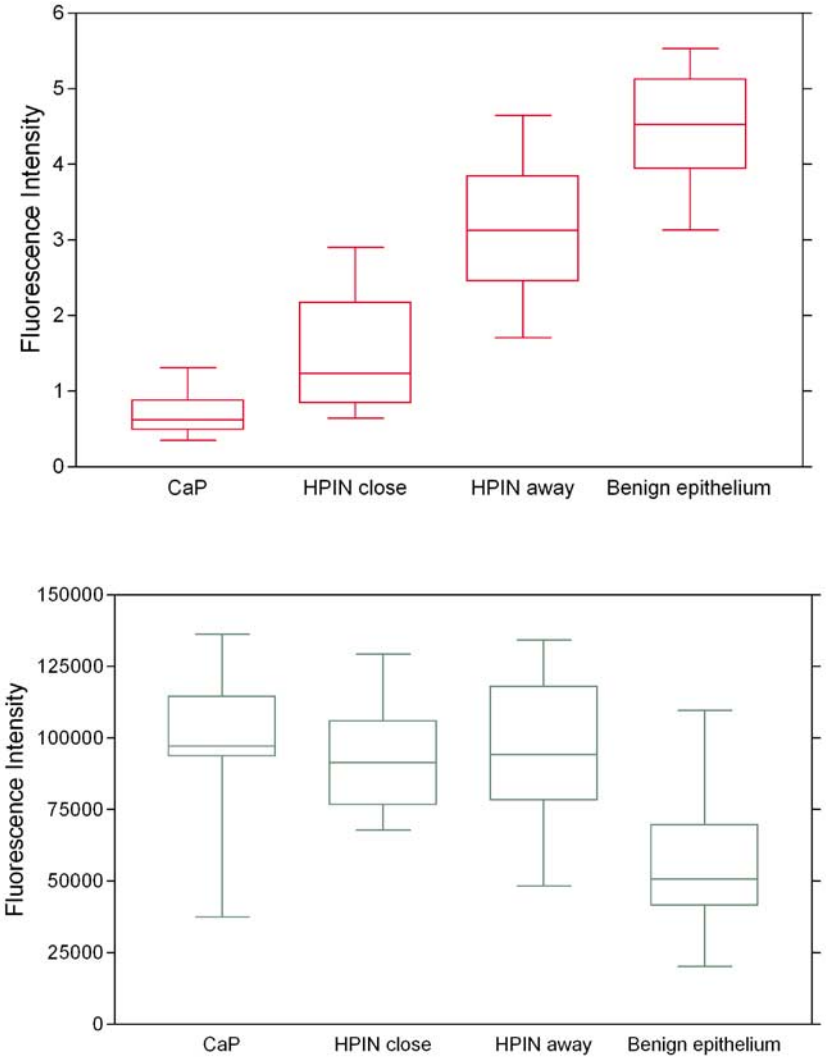

Figure 2 Distribution of total telomeric (**a**) and centromeric (**b**) signal intensities for four regions of interest, averaged over 15 patients is shown. All error bars represent a value of one s.d. from the mean. Significant loss of telomeric signal is observed in regions of HPIN and CaP in comparison with normal prostate epithelium. Telomere length further differentiated HPIN foci situated near CaP from those situated away from CaP ($\geqslant$2 mm). In parallel, total centromeric intensities indicate change in ploidy in HPIN and CaP at similar levels in comparison with benign epithelium

normal prostate epithelium. Further analysis of the distribution of centromeric values in these lesions shows that 30–70% of cells have centromeric values approximating triploid and tetraploid values in comparison with normal prostate epithelium (Figure 4). Although higher percentage of tetraploid cells is expected in populations with increased proliferative activity, this alone cannot account for the increase in total centromere intensity seen in these eight patients.

Numerical chromosomal changes for chromosomes 7, 8 and Y were analysed using interphase FISH in a subset of eight samples. Numeric chromosomal aberrations including gain or loss of one or more chromosomes were found in 38% of CaP foci (three out of eight) and 25% of HPIN foci (two out of eight) situated near CaP (Table 2). In contrast, no numerical changes were observed in benign tissue and HPIN foci situated away from CaP. Gain of chromosome 8 was the most frequent change in both HPIN and CaP, followed by gain of chromosome 7.

Although the comparison of telomeric values in the subset of eight samples follows the same trends of telomere reduction in foci of HPIN and CaP averaged over 15 samples, the comparison of telomere lengths between different foci of CaP in samples showing numerical chromosomal abnormalities *versus* those that do not, does not reach statistical significance. This is to be expected in the light of the small sample size used in comparison ($n=3$ aneuploid *versus* $n=5$ diploid CaP foci by interphase FISH).

Immunohistochemical analysis of p53 levels was also performed, and the results are summarized in Table 2. High levels of p53 (consistent with p53 mutation (Baas *et al*., 1994)) were observed in CaP and HPIN situated adjacent to CaP in two out of eight patients. The same foci also showed evidence of aneusomy by interphase

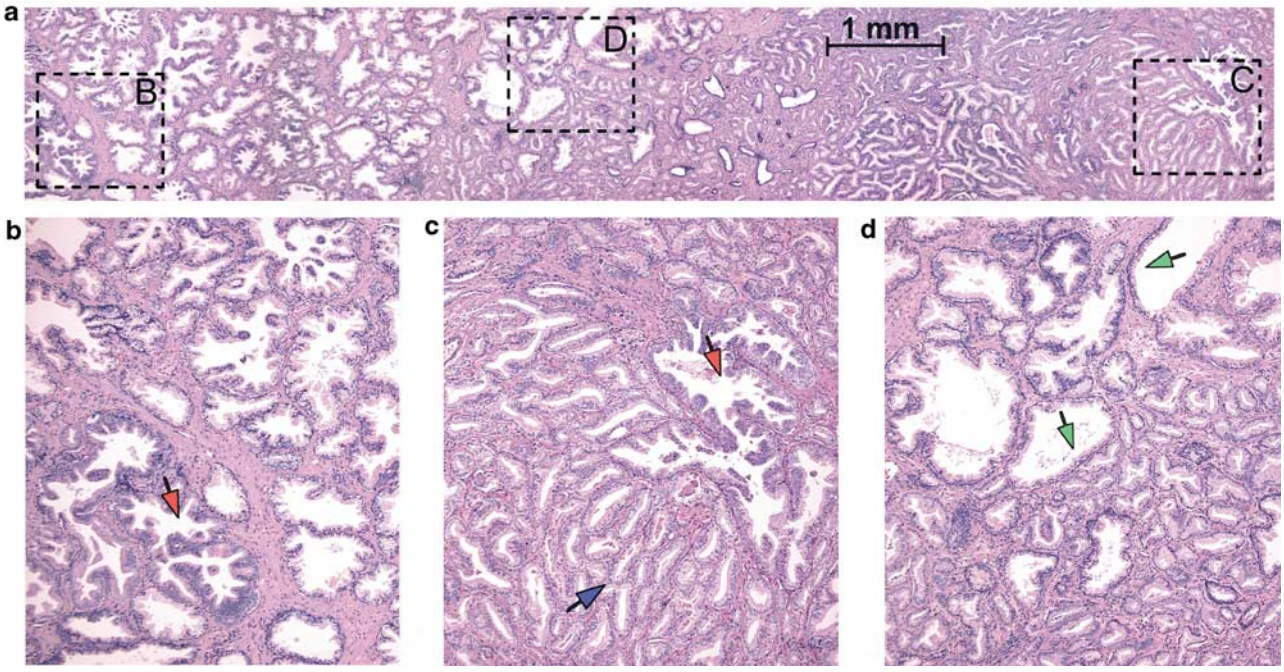

Figure 3 H&E composite image of regions of interest used in the study is shown (**a**). For each patient, representative regions of HPIN (red arrows), CaP (blue arrow) and normal (benign) prostate epithelium (green arrows) were analysed. Two foci of HPIN were examined per patient and differed in their proximity to concurrent CaP. Representative H&E images of HPIN situated near (**c**) and away from CaP were at no times more than 2 mm away from it (0.5 ± 0.6 mm). Average distance of HPIN situated away from CaP was 6.8 ± 2.1 mm. Owing to scarcity of the benign tissue in the available sections, multiple foci of normal prostatic epithelium at varying distance to carcinoma were analysed (**d**) to obtain sufficient number of cells averaged over 15 patients, this distance was 4.3 ± 4.6 mm

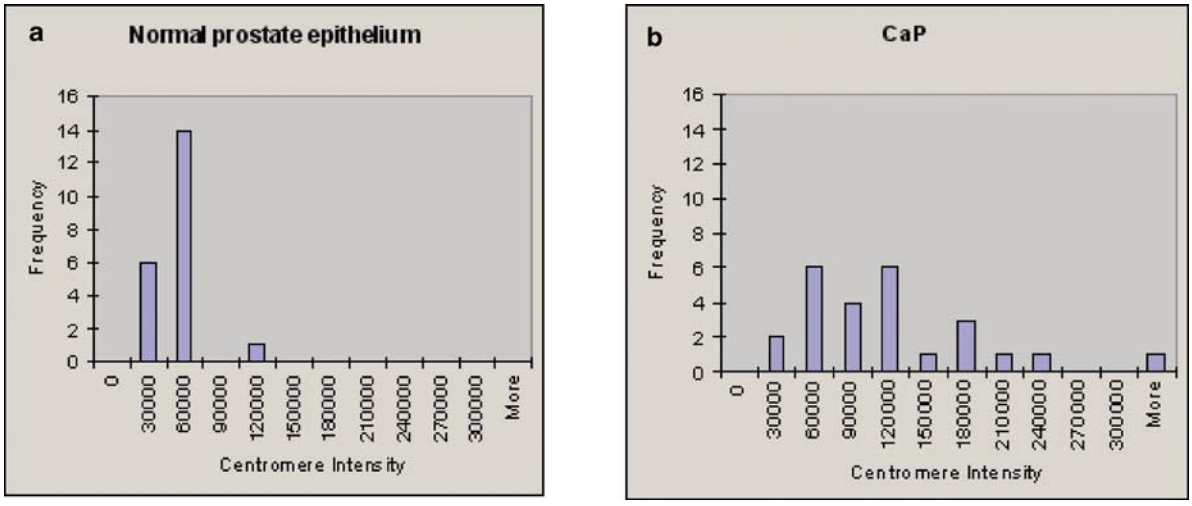

Figure 4 Representative distribution of centromere intensities in normal (benign) epithelium (**a**) and cancer focus (**b**). Distribution of centromeric intensities in normal prostate epithelium is taken as a crude measure of a diploid karyotype. Diploidy of normal epithelium is confirmed in interphase FISH analysis (no gains or losses of 7, 8 and Y). Cancer focus displays a wider distribution of centromeric intensities indicating heterogeneity and possible instability. Distribution suggests presence of an aneuploid as well as a high percentage of tetraploid cells in at least a subset of cancers (eight out of 15)

FISH. Benign tissue and HPIN situated away from CaP did not show p53 expression.

Analysis of proliferative rates of individual foci was performed by immunohistochemistry with the established proliferative marker Ki-67. An increased number of proliferating cells was observed in HPIN and CaP in comparison with normal prostatic epithelium and reached significant levels at $P < 0.05$ in carcinoma and HPIN situated near CaP (Figure 5). There was no significant correlation of patient age, pathological staging parameters or Gleason score (Table 1) to the above findings including telomeric and centromeric intensities, proliferative activity or p53 status.

Table 2 Summary of interphase FISH analysis and p53 immunostaining on the subset of eight patients

Tissue area examined	*Numerical chromosome abnormalities*	*p53 immunostaining*	*Intensity relative to normal epithelium*	
			Telomere	*Centromere*
Benign	0/8 (0%)	0/8 (0%)	1.00	1.00
HPIN away from CaP	0/8 (0%)	0/8 (0%)	0.66	1.64
HPIN near CaP	2/8 (25%)[a]	2/8 (25%)[a]	0.35	1.62
CaP	3/8 (38%)[a]	2/8 (25%)[a]	0.16	1.90

[a]All of the p53 positive samples have shown presence of numerical chromosomal abnormalities

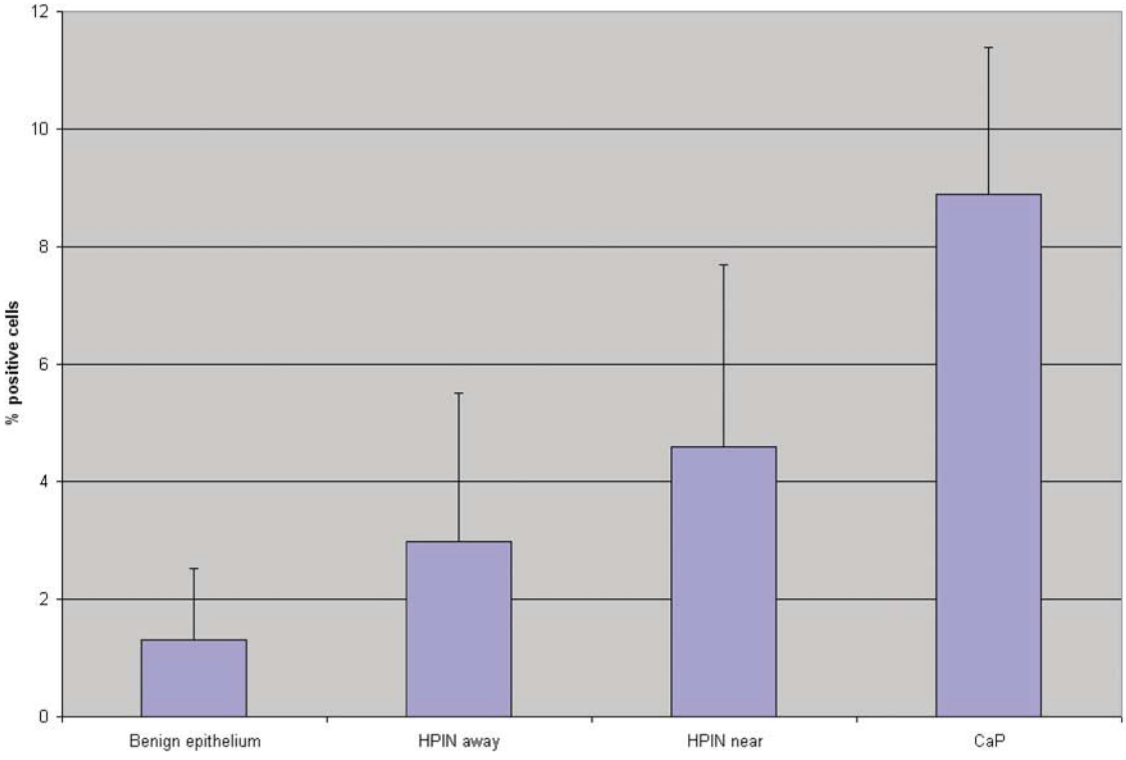

Figure 5 Relative proliferation rates in the regions of interest, expressed as a percentage of Ki-67 positive cells averaged over 15 specimens are shown. Increase in proliferative rates in HPIN and CaP is observed in comparison with normal prostate epithelium and reaches significance in CaP and HPIN situated near it

Discussion

CaP typically affects older men. Therefore, it is of great interest that a cellular process considered to be a determinant of age-dependent senescence is implicated in CaP oncogenesis. Based on the findings of this study, we propose that telomere erosion may be an important cellular risk factor for older men exhibiting HPIN.

Loss of telomeric ends has previously been shown in CaP cell lines and has been studied in a limited number of reports using patient tissue samples (Koeneman *et al*., 1998; Zhang *et al*., 1998). Little is currently known about the distribution of telomere lengths in different grades and stages of CaP progression mainly because of difficulties in obtaining sufficient histologically pure tissue that is representative of benign, preneoplastic (HPIN) or CaP. Furthermore, owing to the multifocal nature and intermingling histology of both HPIN and CaP (Cheng *et al*., 1998), genotypic differences between different foci are often lost during the bulk extraction procedures required to obtain sufficient tissue for both telomere and telomerase analyses. Q-FISH analysis allows for cell-to-cell analysis and quantification of intracellular variation of different lesions within the same tissue section. In addition, areas of interest can be directly compared to the most appropriate internal control, concurrent benign tissue. Another advantage is that parallel tissue sections of an area of interest can usually be studied to provide more integrative analyses. In an example of such sequential analyses, it was recently found that telomere signal intensities in cells from tissue sections correlated with telomere length as assessed by telomere restriction fragment (TRF) analysis (Meeker *et al*., 2002).

In this study, we applied the above method to compare the relative changes in telomere size in representative areas of benign, HPIN and CaP histology. The distribution of telomere signals in all the 15 patients indicated that there was a significant reduction in telomere signal intensity in areas of CaP and HPIN with respect to concurrent benign tissue. Furthermore, a detailed analysis of telomere length distribution within HPIN foci suggested that there was a topographical relation between these lesions such that HPIN situated immediately adjacent to CaP had telomere intensity values reflecting a length that was closer to that of carcinoma than was the case for HPIN found away (>3 mm) from foci of CaP. Interestingly, a more detailed Q-FISH analysis of four different HPIN foci on a subset of CaP patients (not shown) displayed a high degree of variability in centromere and telomere intensities between individual foci. This observation is also in keeping with the multifocal model of CaP oncogenesis (Bostwick *et al*., 1998; Foster *et al*., 2000; Harding and Theodorescu, 2000).

In keeping with the end replication problem, telomere loss is likely to be concomitant with increased proliferative activity (Figure 4). Cell kinetic studies (Bonkhoff *et al*., 1994) have indicated abnormal differentiation and gain of proliferative capacity in CaP and in the secretory epithelial layer of HPIN. To determine whether there was correlation between regional telomere loss and proliferation, parallel sections were examined using antibody against Ki-67 nuclear antigen. An increase in the percentage of cycling cells was observed in CaP and HPIN in comparison with benign epithelium and reached significance in CaP and HPIN situated near CaP, within this study group.

Telomere loss is associated with end-to-end fusion and more generalized chromosomal instability (Muller, 1938; McClintock, 1941; Ducray *et al*., 1999; Hande *et al*., 1999; Artandi and DePinho, 2000). To examine changes in the overall chromosomal content, the total centromeric intensities per cell were analysed. Centromere intensities were found to increase by an average of 40% in HPIN and CaP in comparison with benign tissue. This provides additional support so that the two lesions could be related in origins and give rise to these aberrant ratios, perhaps through tetraploidization and subsequent selective loss of chromosomes (Giaretti and Santi, 1990; Shackney *et al*., 1995; Rasnick and Duesberg, 1999). The distribution of centromeric values in CaP and HPIN in this study indicates the presence of a tetraploid population in at least a portion of HPIN and CaP foci (Figure 4), lending support to the argument that tetraploidy might be an important step in the development of aneuploidy in CaP.

Chromosomal instability and numerical aberrations have been previously observed in CaP cell lines (Beheshti *et al*., 2001) and in patient samples (Cunningham *et al*., 1996; Erbersdobler *et al*., 1999; Al-Maghrabi *et al*., 2001, 2002). Little is known about mechanisms driving the generation of excess aberrations during CaP development and progression. Telomere dysfunction, although likely, is not the only mechanism that can explain increase in aneusomy levels observed in HPIN and CaP. Alternate mechanisms could include defects in DNA repair (reviewed in Coleman and Tsongalis (1995), Morgan *et al*. (1998), Hixon and Gualberto (2000)) as well as errors in the mitotic segregation machinery (Elledge, 1996 #149) and oxidative stress (Bohr *et al*., 1998). In a subset of tissues studied, foci of CaP and HPIN situated adjacent to CaP not only developed numerical chromosomal aberrations, but also expressed high levels of p53 detected with an antibody previously (Baas *et al*., 1994), but not exclusively (Campbell *et al*., 1993) associated with p53 mutation. These data suggested that CaP may be associated with progression of certain HPIN foci harboring p53 mutation and/or numerical chromosomal aberrations. Thus, a circumstantial relation between p53 mutation, telomere length erosion and generation of chromosomal instability seems probable. Further studies on a larger patient cohort will be required to determine the precise role and prognostic value of telomere erosion in histologic tissue sections of men with persistent HPIN.

Materials and methods

Tissue accrual

Patient samples used in this study were obtained from radical prostatectomies performed at The University Health Network (UHN), Toronto, over the period of 1995–1997. Study was approved by the institutional ethical review board. Tissue samples were excised from the prostate, formalin fixed and paraffin embedded. The cohort consisted of 15 cases selected on the basis of presence of CaP and multiple foci of HPIN situated at varying distances from areas of CaP. For each specimen, adjacent blocks of tissue flanking the block under study were examined to ensure that no CaP was present adjacent to areas of HPIN defined as being distant from CaP. Serial sections, 5 μm in thickness, were obtained from the blocks. Hematoxylin and eosin (H&E) staining was used to identify the regions of interest including: (1) nondysplastic, hereafter referred to as 'normal' benign epithelial tissue, foci of (2) HPIN and (3) CaP (Figure 1a). Regions of HPIN were further subdivided into (a) foci immediately adjacent to (≤ 2 mm from CaP, 0.5 ± 0.6 mm average distance) or intermingled with CaP foci and (b) foci situated away from CaP (including foci furthest away from CaP in a section, 6.8 ± 2.1 mm on average) (Figure 3).

These regions were examined for telomeric and centromeric DNA content using Q-FISH. In parallel, proliferative activity was assessed using immunohistochemistry for Ki-67 antigen. Eight of the 15 specimen tissue sections were previously analysed for the presence of numerical chromosomal changes of chromosomes 7, 8 and Y, and expression of mutant p53 (Al-Maghrabi *et al*., 2001).

Q-FISH

Q-FISH was performed using pan-telomeric and pan-centromeric PNA probes on unstained, 5 μm sections. Telomere $(C_3TA_2)_3$-and centromere (16-mer α repeat DNA)-specific probes directly labeled with a Cy3 and FITC fluorescent dyes, respectively, were obtained from Boston Probes Inc. The

standard technique for PNA FISH (Poon *et al*., 1999) has been applied with some modifications. Briefly, sections were deparaffinized in xylene (3 × 8 min) and dehydrated with 100% EtOH (3 × 8 min). Slides were incubated with 100 μg/ml RNase in 2 × SSC at 37°C for 60 min, washed with 2 × SSC for 2 min and treated with 1 M NaSCN for 8 min at 80°C. After washing with deionized H_2O, the sections were digested in 5 mg/ml pepsin solution in 0.6% NaCl (pH 1.5) for 8 min at 45°C and rinsed in 2 × SSC at room temperature for 5 min. Slides were further treated with 0.1 M triethanolamine, rinsed with 1 × PBS and 2 × SSC for 10 min, dehydrated through ethanol series (70, 90 and 100%) and air-dried.

A mixture of 20 μl of the telomeric and centromeric probes was applied to the sections to give a final probe concentration of 0.5 μg/ml in each case. Coverslips were placed on areas of interest and sealed with rubber cement. Slides were denatured on a preheated block set at 80°C for 3 min, transferred to a humidified chamber and hybridized in the dark for an hour at 25°C. Coverslips were removed and the slides were washed twice in formamide solution for 15 min (70% formamide, 10 mM Tris, 0.1% BSA, pH = 7.0–7.5) followed by three washes in Tween solution (1 M Tris, 0.15 M NaCl, 0.08% Tween, pH = 7.0–7.5), 5 min each. Slides were counterstained with DAPI/antifade mixture (Vectashield Burlingame, CA, USA) and analysed. Only tissue sections with a hybridization efficiency of >95% were included in the study.

Image capturing

Regions of interest were determined on the parallel H&E sections and identified on the FISH slides using DAPI channel to minimize exposure in Cy3 and FITC channels. Slides were then analysed with a Zeiss Axiophot II epifluorescence microscope equipped with a mercury lamp and a ×100/1.4 N.A. oil immersion lens. Images were captured using a CCD camera and Isis FISH imaging software (Metasystems, GmbH, Germany). In order to compensate for the cell thickness, three consecutive images at different focal depths (average of 1 μm (micron) separation) were stacked into a composite image used for quantitation. Bleaching effects because of repeated exposure of a selected area during image capture were assessed and intensity loss of ~1% was found between exposures. Exposure times were optimized with respect to the intensities of the telomere and centromere signals to prevent the overexposure/saturation of the signals in the original and stacked images. Once determined, they were kept constant for all slides to ensure consistency in intensity measurements. For each slide batch, a control prostate tissue section was processed without the inclusion of PNA probes to ensure that there was no variation in fluorescence due to the pretreatment protocol. An average of 20 cells were examined on adjacent sections to quantify the telomeric and centromeric signals using Q-FISH on each of the 15 specimens.

Image analysis

Quantitative analysis of the telomere/centromere signal intensities was performed on the captured images and used to determine relative changes in telomere length and DNA ploidy. Original 8-bit images of each channel were exported from Metasystems into Adobe Photoshop where cell border were defined based on the DAPI nuclear outline. Images of individual nuclei were then exported and analysed quantitatively using ImageJ software. Quantitative analysis was performed on a per nucleus basis, on Cy3 and FITC images using simple thresholding function to outline the signals. The intensities of all pixels outlined by the threshold were summed up on a per cells basis and tabulated. Since ploidy changes are commonly observed in both CaP and HPIN, all telomere intensities were expressed as a ratio of telomeric-to-centromeric signals for each nucleus. Centromeric intensities were used as a measure of gross ploidy changes. Telomeric ratios and centromeric intensities were then averaged between cells of each region of interest and regions compared using ANOVA in Excel followed by SNK test.

Immunohistochemical analysis of Ki-67

Serial sections parallel to those used for telomere/centromere FISH analyses were used. Proliferative activity of the cells was assessed using monoclonal MIB1 antibody (Coulter-Immunotech) to determine the percentage of cells positive for Ki-67 nuclear antigen. Briefly, slides were dewaxed in xylene for 15 min and hydrated in ethanol series (100, 90 and 70%) followed by the 3% hydrogen peroxide treatment for 15 min to quench endogenous peroxidases. Sections were placed in 10 mM citrate buffer (pH 6.0) in a pressure cooker for 5 min after reaching pressure. Slides were blocked with 5% normal goat serum for 10 min and incubated with the primary antibody at 1 : 200 dilution in antibody dilution buffer (Dako Diagnostics, Canada) for 60 min at 25°C. After rinsing in PBS, slides were incubated with biotinylated secondary antibody (Signet multi-link, Signet Laboratories Inc., MA, USA) for 20 min at 25°C. Detection of the bound antibody was carried out using streptavidin/HRP conjugate for 20 min. NovaRed (Vector Labs, CA, USA) was used as a chromogen followed by the counterstain in Mayer's hematoxylin and mounting with permount.

Paraffin sections of actively proliferating tonsil tissue served as a positive control. Prostate sections processed without secondary antibody and brain tissue were used as negative controls. Areas with highest percentage of positive cells were captured under a bright field microscope and the cells counted. A total of ~1200 cells/slide or 300 cells per focus for each patient was examined and proliferative activity presented as a percentage of MIB-1 positive cells. Nuclear staining, regardless of the intensity was counted as positive for the presence of Ki-67 antigen and proliferative activity.

Interphase FISH analysis of numerical chromosomal changes

Interphase FISH analysis on centromeres of chromosomes 7, 8 and Y was previously performed (published in Al-Maghrabi *et al*., 2001) on eight out of 15 specimens. Slide pretreatment and FISH were done as per the manufacturer's instructions (Vysis Inc., II, USA). Directly labeled centromere enumeration probes for chromosomes 7, 8 and Y were used. Analysis was performed on 5 μm tissue sections from the same tissue block as used for telomere/centromere quantitation and analysis of proliferative activity. A total of 100 nuclei per focus of interest were counted for each probe, up to 400 nuclei per patient. Scoring criteria have been described in detail in Al-Maghrabi *et al*. (2001).

Immunohistochemical analysis of p53

Immunohistochemistry was performed on serial sections from the same paraffin blocks used above. Well-established monoclonal antibody to p53 (DO7 clone; Novocastra Laboratories Ltd, Newcastle, England) (Bonsing *et al*., 1997) was applied

and detected using avidin–biotin peroxidase complex (Elite kit; Vector Laboratories, Burligame, CA, USA). The positive controls for p53 immunoreactivity were formalin-fixed sections from an adenocarcinoma of breast and bladder transitional cell carcinoma. Stromal cells were used as negative internal controls.

Acknowledgements
We thank Jana Karaskova, Ilan Braude, Jane Bayani and Lada Vorobyova for their technical expertise. We also thank Dr Lea Harrington and Dr Salomon Minkin for critical discussions and review. This research is supported by the Canadian Prostate Cancer Research Initiative.

References

Al-Maghrabi J, Vorobyova L, Chapman W, Jewett M, Zielenska M and Squire JA. (2001). *Mod. Pathol.*, **14,** 1252–1262.
Al-Maghrabi J, Vorobyova L, Toi A, Chapman W, Zielenska M and Squire JA. (2002). *Arch. Pathol. Lab. Med.*, **126,** 165–169.
Artandi SE and DePinho RA. (2000). *Curr. Opin. Genet. Dev.*, **10,** 39–46.
Baas IO, Mulder JW, Offerhaus GJ, Vogelstein B and Hamilton SR. (1994). *J. Pathol.*, **172,** 5–12.
Bastacky SI, Wojno KJ, Walsh PC, Carmichael MJ and Epstein JI. (1995). *J. Urol.*, **153,** 987–992.
Beheshti B, Park PC, Sweet JM, Trachtenberg J, Jewett MA and Squire JA. (2001). *Neoplasia.*, **3,** 62–69.
Bohr V, Anson RM, Mazur S and Dianov G. (1998). *Toxicol. Lett.*, **102–103, 47–52.**
Bonkhoff H, Stein U and Remberger K. (1994). *Prostate*, **24,** 114–118.
Bonsing BA, Corver WE, Gorsira MC, van Vliet M, Oud PS, Cornelisse CJ and Fleuren GJ. (1997). *Cytometry*, **28,** 11–24.
Bostwick DG, Shan A, Qian J, Darson M, Maihle NJ, Jenkins RB and Cheng L. (1998). *Cancer*, **83,** 1995–2002.
Campbell C, Quinn AG, Angus B and Rees JL. (1993). *Br. J. Dermatol.*, **129,** 235–241.
Cheng L, Song SY, Pretlow TG, Abdul-Karim FW, Kung HJ, Dawson DV, Park WS, Moon YW, Tsai ML, Linehan WM, Emmert-Buck MR, Liotta LA and Zhuang Z. (1998). *J. Natl. Cancer Inst.*, **90,** 233–237.
Coleman WB and Tsongalis GJ. (1995). *Clin Chem.*, **41,** 644–657.
Counter CM. (1996). *Mutat. Res.*, **366,** 45–63.
Cunningham JM, Shan A, Wick MJ, McDonnell SK, Schaid DJ, Tester DJ, Qian J, Takahashi S, Jenkins RB, Bostwick DG and Thibodeau SN. (1996). *Cancer Res.*, **56,** 4475–4482.
Dong JT, Isaacs WB and Isaacs JT. (1997). *Curr. Opin. Oncol.*, **9,** 101–107.
Ducray C, Pommier JP, Martins L, Boussin FD and Sabatier L. (1999). *Oncogene*, **18,** 4211–4223.
Emmert-Buck MR, Vocke CD, Pozzatti RO, Duray PH, Jennings SB, Florence CD, Zhuang Z, Bostwick DG, Liotta LA and Linehan WM. (1995). *Cancer Res.*, **55,** 2959–2962.
Erbersdobler A, Bardenhagen P and Henke RP. (1999). *Prostate*, **38,** 92–99.
Erbersdobler A, Gurses N and Henke RP. (1996). *Pathol. Res. Pract.*, **192,** 418–427.
Foster CS, Bostwick DG, Bonkhoff H, Damber JE, van der Kwast T, Montironi R and Sakr WA. (2000). *Scand. J. Urol. Nephrol. Suppl.*, 19–43.
Giaretti W and Santi L. (1990). *Int. J. Cancer*, **45,** 597–603.
Goyns MH and Lavery WL. (2000). *Mech. Ageing Dev.*, **114,** 69–77.
Graham Jr SD, Bostwick DG, Hoisaeter A, Abrahamsson P, Algaba F, di Sant'Agnese A, Mostofi FK and Napalkov P. (1992). *Cancer*, **70,** 359–361.
Grobelny JV, Kulp-McEliece M, Broccoli D. (2001). *Hum. Mol. Genet.*, **10,** 1953–1961.
Haas GP and Sakr WA. (1997). *CA Cancer J. Clin.*, **47,** 273–287.
Hande MP, Samper E, Lansdorp P and Blasco MA. (1999). *J. Cell Biol.*, **144,** 589–601.
Harding MA and Theodorescu D. (2000). **5,** 258–264.
Harley CB. (1991). *Mutat. Res.*, **256,** 271–282.
Hixon ML and Gualberto A. (2000). *Front Biosci.*, **5,** D50–D57.
Isaacs WB, Bova GS, Morton RA, Bussemakers MJ, Brooks JD and Ewing CM. (1994). *Semin. Oncol.*, **21,** 514–521.
Kallakury BV, Brien TP, Lowry CV, Muraca PJ, Fisher HA, Kaufman Jr RP and Ross JS. (1997). *Diag. Mol. Pathol.*, **6,** 192–198.
Koeneman KS, Pan CX, Jin JK, Pyle III JM, Flanigan RC, Shankey TV and Diaz MO. (1998). *J. Urol.*, **160,** 1533–1539.
Lin Y, Uemura H, Fujinami K, Hosaka M, Harada M and Kubota Y. (1997). *J. Urol.*, **157,** 1161–1165.
Macoska JA, Trybus TM, Sakr WA, Wolf MC, Benson PD, Powell IJ and Pontes JE. (1994). *Cancer Res.*, **54,** 3824–3830.
McClintock B. (1941). *Genetics*, **26,** 234–282.
McNeal J and Bostwick DG. (1986). *Hum. Pathol.*, **17**.
Meeker AK, Gage WR, Hicks JL, Simon I, Coffman JR, Platz EA, March GE and De Marzo AM. (2002). *Am. J. Pathol.*, **160,** 1259–1268.
Morgan WF, Corcoran J, Hartmann A, Kaplan MI, Limoli CL and Ponnaiya B. (1998). *Mutat. Res.*, **404,** 125–128.
Muir CS, Nectoux J and Staszewski J. (1991). *Acta Oncol.*, **30,** 133–140.
Muller H. (1938). *Collecting Net*, **13,** 183–195.
Olovnikov AM. (1973). *J. Theor. Biol.*, **41,** 181–190.
Poon SS, Martens UM, Ward RK and Lansdorp PM. (1999). *Cytometry*, **36,** 267–278.
Qian J, Jenkins RB and Bostwick DG. (1995). *Urology*, **46,** 837–842.
Qian J, Jenkins RB and Bostwick DG. (1999). *Eur. Urol.*, **35,** 479–483.
Rasnick D and Duesberg PH. (1999). *Biochem. J.*, **340 (Part 3), 621–630.**
Sakr WA and Grignon DJ. (1998). *Anal. Quant. Cytol. Histol.*, **20,** 417–423.
Sakr WA, Grignon DJ, Haas GP, Heilbrun LK, Pontes JE and Crissman JD. (1996). *Eur. Urol.*, **30,** 138–144.
Sakr WA, Grignon DJ, Haas GP, Schomer KL, Heilbrun LK, Cassin BJ, Powell J, Montie JA, Pontes JE and Crissman JD. (1995). *Pathol. Res. Pract.*, **191,** 838–841.
Sakr WA, Haas GP, Cassin BF, Pontes JE and Crissman JD. (1993). *J. Urol.*, **150,** 379–385.
Sakr WA and Partin AW. (2001). *Urology*, **57,** 115–120.
Scates DK, Muir GH, Venitt S and Carmichael PL. (1997). *Br. J. Urol.*, **80,** 263–268.
Shackney SE, Berg G, Simon SR, Cohen J, Amina S, Pommersheim W, Yakulis R, Wang S, Uhl M, Smith CA, Pollice AA and Hartstock RJ. (1995). *Cytometry*, **22,** 307–316.

Takahashi C, Miyagawa I, Kumano S and Oshimura M. (1997). *Eur. Urol.*, **32,** 494–498.

Takahashi S, Alcaraz A, Brown JA, Borell TJ, Herath JF, Bergstralh EJ, Lieber MM and Jenkins RB. (1996). *Clin. Cancer Res.*, **2,** 137–145.

van der Kwast TH, Labrie F and Tetu B. (1999). *Eur. Urol.*, **35,** 508–510.

Wen J, Cong YS and Bacchetti S. (1998). *Hum. Mol. Genet.*, **7,** 1137–1141.

Wullich B, Rohde V, Oehlenschlager B, Bonkhoff H, Ketter R, Zwergel T and Sattler HP. (1999). *J. Urol.*, **161,** 1997–2001.

Zhang W, Kapusta LR, Slingerland JM and Klotz LH. (1998). *Cancer Res.*, **58,** 619–621.